Shear-bulk coupling in nonconformal hydrodynamics

Gabriel S. Denicol
Department of Physics, McGill University, 3600 University Street, Montreal, QC H3A 2T8, Canada

Wojciech Florkowski
Institute of Physics, Jan Kochanowski University, PL-25406 Kielce, Poland
and The H. Niewodniczański Institute of Nuclear Physics, Polish Academy of Sciences, PL-31342 Kraków, Poland

Radoslaw Ryblewski
Department of Physics, Kent State University, Kent, Ohio 44242, USA
and The H. Niewodniczański Institute of Nuclear Physics, Polish Academy of Sciences, PL-31342 Kraków, Poland

Michael Strickland
Department of Physics, Kent State University, Kent, Ohio 44242, USA
(Received 23 July 2014; revised manuscript received 8 September 2014; published 9 October 2014)

We compute the temporal evolution of the pressure anisotropy and bulk pressure of a massive gas using second-order viscous hydrodynamics and anisotropic hydrodynamics. We then compare our results with an exact solution of the Boltzmann equation for a massive gas in the relaxation time approximation. We demonstrate that, within second-order viscous hydrodynamics, the inclusion of the full set of kinetic coefficients, particularly the shear-bulk couplings, is necessary to properly describe the time evolution of the bulk pressure. We also compare the results of second-order hydrodynamics with those obtained using the anisotropic hydrodynamics approach. We find that anisotropic hydrodynamics and second-order viscous hydrodynamics including the shear-bulk couplings are both able to reproduce the exact evolution with comparable accuracy.

DOI: 10.1103/PhysRevC.90.044905 PACS number(s): 12.38.Mh, 24.10.Nz, 25.75.−q, 51.10.+y

I. INTRODUCTION

Dissipative hydrodynamics plays a central role in the phenomenology of the quark gluon plasma. Since quantum mechanics implies that there is a lower bound on the shear viscosity to entropy density ratio [1,2], one must include dissipative viscous corrections in order to realistically model the spatiotemporal evolution of the soft degrees of freedom of the system. The application of ideal [3–5] and second-order viscous hydrodynamics [6–32] now has a long history with recent developments focusing on constructing complete and self-consistent methods for deriving the fluid-dynamical equations of motion and the associated transport coefficients. Following a different strategy, another promising framework for describing the soft dynamics of relativistic systems has recently been developed called anisotropic hydrodynamics [33–48]. While second-order hydrodynamics is constructed from an expansion around a local equilibrium state, anisotropic hydrodynamics originates from an expansion around a dynamically evolving anisotropic background.

So far, fluid-dynamical theories that include only the effects of shear viscous corrections have been considered sufficient to describe the strongly interacting system created in ultrarelativistic heavy-ion collisions. However, since QCD is a nonconformal field theory, one should not neglect the bulk viscous corrections to the ideal energy momentum tensor if one wants a complete and self-consistent description of the dynamics. While the accuracy of second-order and anisotropic hydrodynamics has been investigated in the conformal and/or massless limits [49,50], there have not been comparisons of complete second-order formulations in the nonconformal case. It was recently shown that Israel-Stewart theory [51], which is the most widespread formulation of relativistic dissipative fluid dynamics, is not able to reproduce exact solutions of the *massive* 0+one-dimensional (1D) Boltzmann equation in the relaxation time approximation [52]. Therefore, one is led to ask whether more complete formulations of second-order viscous hydrodynamics can better reproduce the exact solution.

In the past several months, some progress has been made in the second-order viscous hydrodynamics framework within the 14-moment approximation [32] and in the anisotropic hydrodynamics framework [53]. Both of these formalisms have been extended to provide a more accurate description of massive and, consequently, nonconformal systems. In Ref. [53] it was shown that inclusion of an explicit bulk degree of freedom in the anisotropic hydrodynamics framework results in a quite reasonable agreement with the exact kinetic solutions. In this paper we take another step in this direction and compare the solutions of second-order hydrodynamics obtained using the 14-moment approximation [32] with the exact kinetic solution from Ref. [52]. We demonstrate that the failure of Israel-Stewart theory in reproducing solutions of the Boltzmann equation in the massive case occurs because this theory does not take into account the coupling between bulk viscous pressure and the shear-stress tensor. We find that, for the case of the bulk viscous pressure, such coupling terms become as important as the corresponding first-order Navier-Stokes term and must be included in order to obtain a reasonable agreement with the microscopic theory. This indicates that the coupling between the two viscous contributions can be relevant in the description of nonconformal fluids.

We further compare the recent solutions of anisotropic hydrodynamics derived in Ref. [53] with those of second-order viscous hydrodynamics. We find that both are able to reproduce the exact solution with comparable accuracy. Such good agreement found between anisotropic hydrodynamics and solutions of the Boltzmann equation is encouraging since in anisotropic hydrodynamics the shear-bulk couplings do not need to be included explicitly but are instead implicit in the formalism.

The structure of this paper is as follows. In Sec. II we present the recently obtained second-order viscous hydrodynamics equations of motion obtained using the 14-moment approximation. In Sec. III we present the necessary 0+1D anisotropic hydrodynamics equations including the bulk degree of freedom. In Sec. IV we briefly review the method for solving the 0+1D massive Boltzmann equation exactly. In Sec. V we present our numerical results. In Sec. VI we present our conclusions and an outlook for the future. In the appendix, we collect expressions for the necessary thermodynamic integrals and their asymptotic expansions.

A. Notation and conventions

We use natural units with $\hbar = c = k_B = 1$. The metric tensor has the form $g^{\mu\nu} = \mathrm{diag}(1,-1,-1,-1)$. The space-time coordinates are denoted as $x^\mu = (t,x,y,z)$, and the longitudinal proper time is $\tau = \sqrt{t^2 - z^2}$.

B. Bulk variables

In order to compare the various approximation schemes considered herein, we will specialize in the end to the case that the equilibrium distribution is a classical massive Boltzmann distribution. In this case, the isotropic equilibrium bulk variables are

$$n_{\rm eq}(T,m) = 4\pi\tilde{N}T^3\hat{m}_{\rm eq}^2 K_2(\hat{m}_{\rm eq}), \tag{1}$$

$$\mathcal{S}_{\rm eq}(T,m) = 4\pi\tilde{N}T^3\hat{m}_{\rm eq}^2[4K_2(\hat{m}_{\rm eq}) + \hat{m}_{\rm eq}K_1(\hat{m}_{\rm eq})], \tag{2}$$

$$\mathcal{E}_{\rm eq}(T,m) = 4\pi\tilde{N}T^4\hat{m}_{\rm eq}^2[3K_2(\hat{m}_{\rm eq}) + \hat{m}_{\rm eq}K_1(\hat{m}_{\rm eq})], \tag{3}$$

$$\mathcal{P}_{\rm eq}(T,m) = n_{\rm eq}(T,m)\,T, \tag{4}$$

where $n_{\rm eq}, \mathcal{S}_{\rm eq}, \mathcal{E}_{\rm eq}$, and $\mathcal{P}_{\rm eq}$ are the equilibrium number density, entropy density, energy density, and pressure, respectively, $\hat{m}_{\rm eq} = m/T$, and $\tilde{N} = N_{\rm dof}/(2\pi)^3$ with $N_{\rm dof}$ being the number of degrees of freedom.

II. 14-MOMENT APPROXIMATION APPROACH TO FLUID DYNAMICS

Using the 14-moment approximation one can derive the equations of motion for a relativistic fluid from the relativistic Boltzmann kinetic equation. In this way, the continuity equations for the energy-momentum tensor

$$\partial_\mu T^{\mu\nu} = 0, \tag{5}$$

have to be solved together with the relaxation-type equations for the bulk viscous pressure Π and the shear-stress tensor $\pi^{\mu\nu}$ [32],

$$\tau_\Pi\dot{\Pi} + \Pi = -\zeta\theta - \delta_{\Pi\Pi}\Pi\theta + \varphi_1\Pi^2 + \lambda_{\Pi\pi}\pi^{\mu\nu}\sigma_{\mu\nu} + \varphi_3\pi^{\mu\nu}\pi_{\mu\nu}, \tag{6}$$

$$\tau_\pi\dot{\pi}^{\langle\mu\nu\rangle} + \pi^{\mu\nu} = 2\eta\sigma^{\mu\nu} + 2\tau_\pi\pi_\alpha^{\langle\mu}\omega^{\nu\rangle\alpha} - \delta_{\pi\pi}\pi^{\mu\nu}\theta + \varphi_7\pi_\alpha^{\langle\mu}\pi^{\nu\rangle\alpha} - \tau_{\pi\pi}\pi_\alpha^{\langle\mu}\sigma^{\nu\rangle\alpha} + \lambda_{\pi\Pi}\Pi\sigma^{\mu\nu} + \varphi_6\Pi\pi^{\mu\nu}. \tag{7}$$

Here we have neglected the effect of net-charge diffusion. Above, we introduced the vorticity tensor $\omega_{\mu\nu} \equiv (\nabla_\mu u_\nu - \nabla_\nu u_\mu)/2$, the shear tensor $\sigma_{\mu\nu} \equiv \nabla_{\langle\mu}u_{\nu\rangle}$, and the expansion scalar $\theta \equiv \nabla_\mu u^\mu$, where u^μ is the fluid four-velocity and $\nabla_\mu \equiv \Delta^\nu_\mu\partial_\nu$ is the projected spatial gradient. We use the notation $A^{\langle\mu\nu\rangle} \equiv \Delta^{\mu\nu}_{\alpha\beta}A^{\alpha\beta}$, with $\Delta^{\mu\nu}_{\alpha\beta} \equiv (\Delta^\mu_\alpha\Delta^\nu_\beta + \Delta^\mu_\beta\Delta^\nu_\alpha - 2/3\Delta^{\mu\nu}\Delta_{\alpha\beta})/2$, where $\Delta^{\mu\nu} \equiv g^{\mu\nu} - u^\mu u^\nu$. In Eqs. (6) and (7) we have also introduced the shorthand notation for the proper-time derivative $\dot{(\,)} \equiv d/d\tau$.

The terms multiplying different tensor structures in (6) and (7) are transport coefficients. They are complicated functions of temperature and the particle's mass, and their form should be found by matching (6) and (7) with the underlying microscopic theory. As shown in Ref. [54], the terms $\varphi_1\Pi^2$, $\varphi_3\pi^{\mu\nu}\pi_{\mu\nu}$, $\varphi_6\Pi\pi^{\mu\nu}$, and $\varphi_7\pi_\alpha^{\langle\mu}\pi^{\nu\rangle\alpha}$ appear only because the collision term is nonlinear in the single-particle distribution function. In the case of the relaxation time approximation, which will be employed throughout this paper, the collision term is assumed to be linear in the nonequilibrium single-particle distribution function and one can explicitly show that $\varphi_1 = \varphi_3 = \varphi_6 = \varphi_7 = 0$. One should stress, however, that Eqs. (6) and (7) include a coupling between the shear and bulk relaxation equations (the terms $\lambda_{\Pi\pi}$ and $\lambda_{\pi\Pi}$), which are absent in the traditional Israel-Stewart viscous hydrodynamics. One can find a plot of the various transport coefficients in Fig. 1 of Ref. [32]. There have been some prior works that have considered shear-bulk couplings in viscous hydrodynamics, see, e.g., Refs. [55–57], but for the most part, the existence of these types of couplings has been ignored in the literature.

In the 0+1D case describing one-dimensional and boost-invariant expansion, the formulas (5)–(7) reduce to

$$\dot{\mathcal{E}} = -\frac{\mathcal{E} + \mathcal{P} + \Pi - \pi}{\tau}, \tag{8}$$

$$\tau_\Pi\dot{\Pi} + \Pi = -\frac{\zeta}{\tau} - \delta_{\Pi\Pi}\frac{\Pi}{\tau} + \lambda_{\Pi\pi}\frac{\pi}{\tau}, \tag{9}$$

$$\tau_\pi\dot{\pi} + \pi = \frac{4}{3}\frac{\eta}{\tau} - \left(\frac{1}{3}\tau_{\pi\pi} + \delta_{\pi\pi}\right)\frac{\pi}{\tau} + \frac{2}{3}\lambda_{\pi\Pi}\frac{\Pi}{\tau}, \tag{10}$$

where $\mathcal{E}$ and $\mathcal{P}$ are the energy density and thermodynamic pressure, respectively. We note that in 0+1D the vorticity tensor vanishes and the term $2\tau_\pi\pi_\alpha^{\langle\mu}\omega^{\nu\rangle\alpha}$ has no effect on the dynamics of the fluid. The coefficients appearing in the equation for the bulk pressure are the following:

$$\frac{\zeta}{\tau_\Pi} = \left(\frac{1}{3} - c_s^2\right)(\mathcal{E} + \mathcal{P}) - \frac{2}{9}(\mathcal{E} - 3\mathcal{P}) - \frac{m^4}{9}I_{-2,0}, \tag{11}$$

$$\frac{\delta_{\Pi\Pi}}{\tau_\Pi} = 1 - c_s^2 - \frac{m^4}{9}\gamma_2^{(0)}, \tag{12}$$

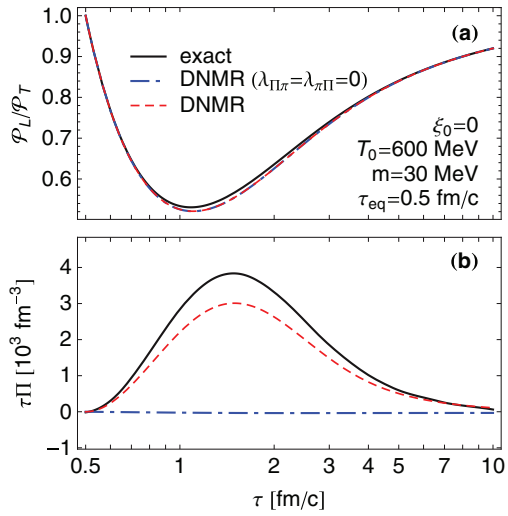

FIG. 1. (Color online) Time evolution of the pressure anisotropy $\mathcal{P}_L/\mathcal{P}_T$ (a) and the bulk pressure (b). Three lines describe three different results: the exact solution of the Boltzmann equation [52] (black solid line), the result of the full second-order viscous hydrodynamics [32] including the shear-bulk couplings $\lambda_{\Pi\pi}$ and $\lambda_{\pi\Pi}$ (red dashed line), and the result of the second-order hydrodynamics with $\lambda_{\Pi\pi} = \lambda_{\pi\Pi} = 0$ (blue dot-dashed line). For both panels we use $m = 30$ MeV, $\tau_0 = 0.5$ fm/c, $\tau_{\rm eq} = \tau_\pi = \tau_\Pi = 0.5$ fm/c, and $T_0 = 600$ MeV. The initial spheroidal anisotropy parameter fixing the initial distribution function equals $\xi_0 = 0$, correspondingly, we use $\pi_0 = 0$ and $\Pi_0 = 0$.

$$\frac{\lambda_{\Pi\pi}}{\tau_\Pi} = \frac{1}{3} - c_s^2 + \frac{m^2}{3}\gamma_2^{(2)}. \tag{13}$$

On the other hand, the coefficients in the equation for the shear pressure are

$$\frac{\eta}{\tau_\pi} = \frac{4}{5}\mathcal{P} + \frac{1}{15}(\mathcal{E} - 3\mathcal{P}) - \frac{m^4}{15}I_{-2,0}, \tag{14}$$

$$\frac{\delta_{\pi\pi}}{\tau_\pi} = \frac{4}{3} + \frac{1}{3}m^2\gamma_2^{(2)}, \tag{15}$$

$$\frac{\tau_{\pi\pi}}{\tau_\pi} = \frac{10}{7} + \frac{4}{7}m^2\gamma_2^{(2)}, \tag{16}$$

$$\frac{\lambda_{\pi\Pi}}{\tau_\pi} = \frac{6}{5} - \frac{2}{15}m^4\gamma_2^{(0)}, \tag{17}$$

where we have introduced the sound velocity squared,

$$c_s^2 = \frac{\mathcal{E} + \mathcal{P}}{\beta_0 I_{3,0}}, \tag{18}$$

and $\beta_0 = I_{1,0}/\mathcal{P}$. The coefficients $\gamma_n^{(0)}$ and $\gamma_n^{(2)}$ are complicated functions of T and m given by

$$\gamma_n^{(0)} = (E_0 + B_0 m^2)I_{-n,0} + D_0 I_{1-n,0} - 4B_0 I_{2-n,0}, \tag{19}$$

$$\gamma_n^{(2)} = \frac{I_{4-n,2}}{I_{4,2}}, \tag{20}$$

where

$$\frac{D_0}{3B_0} = -4\frac{I_{3,1}I_{2,0} - I_{4,1}I_{1,0}}{I_{3,0}I_{1,0} - I_{2,0}I_{2,0}} \equiv -C_2, \tag{21}$$

$$\frac{E_0}{3B_0} = m^2 + 4\frac{I_{3,1}I_{3,0} - I_{4,1}I_{2,0}}{I_{3,0}I_{1,0} - I_{2,0}I_{2,0}} \equiv -C_1, \tag{22}$$

$$B_0 = -\frac{1}{3C_1 I_{2,1} + 3C_2 I_{3,1} + 3I_{4,1} + 5I_{4,2}}. \tag{23}$$

Here we make use of the thermodynamic functions $I_{n,q}$ defined by the integrals

$$I_{n,q}(T,m) = \frac{1}{(2q+1)!!}\int dK (u_\mu k^\mu)^{n-2q}(-\Delta_{\mu\nu}k^\mu k^\nu)^q f_{0k}, \tag{24}$$

where, herein, the equilibrium distribution function is assumed to be a classical Boltzmann distribution $f_{0k} = \exp(-u_\mu k^\mu/T)$, and the integration measure is $dK = N_{\rm dof}\, d^3k/((2\pi)^3 k^0)$. The relevant integrals $I_{n,q}(T,m)$ are expressed in terms of special functions in the appendix. Finally, in this paper we only consider the Boltzmann equation in the relaxation time approximation. In this case, the shear and bulk relaxation times, τ_π and τ_Π, respectively, are equal to the microscopic relaxation time $\tau_{\rm eq}$, i.e., $\tau_\Pi = \tau_\pi = \tau_{\rm eq}$ [32].[1]

We note here that there are other formulations of second-order hydrodynamics which have different values for the various transport coefficients listed above. For example, if one uses the naive Israel-Stewart theory one has $\tau_{\pi\pi} = 0$. In addition, even using the method of moments one finds that the coefficients depend on the number of moments considered. For example, for a gas of massless particles with constant cross sections, one has $\tau_{\pi\pi} = 134/77$ in the 23-moment approximation and $\tau_{\pi\pi} \simeq 1.69$ in the 32- and 41-moment approximations [28]. In this paper, we will use the coefficients calculated in the 14-moment approximation using the relaxation time approximation [32]. We note that, for the case of the relaxation time approximation, the transport coefficients of hydrodynamics have not been calculated beyond the 14-moment approximation.

Finally, in this context we note that even the form of the bulk pressure evolution equations put forward by different authors differ and, generally speaking, until the recent papers of Denicol *et al.*, no authors included explicit shear-bulk couplings, see, e.g., Refs. [7,9,51,58–61]. As shown in Ref. [52], approaches that do not explicitly include the shear-bulk couplings do not agree with the bulk pressure evolution obtained via exact solution of the Boltzmann equation. The complete 14-moment second-order viscous hydrodynamics equations presented in this section include shear-bulk couplings, $\lambda_{\pi\Pi}$ and $\lambda_{\Pi\pi}$. As we will see in the results section, including these couplings results in much better agreement with the exact kinetic solution compared to Israel-Stewart second-order viscous hydrodynamics.

III. ANISOTROPIC HYDRODYNAMICS APPROACH

Anisotropic hydrodynamics (aHydro) is an alternative framework for obtaining the necessary nonequilibrium

[1] In a more general case the relaxation times for the shear and bulk pressures may differ from each other.

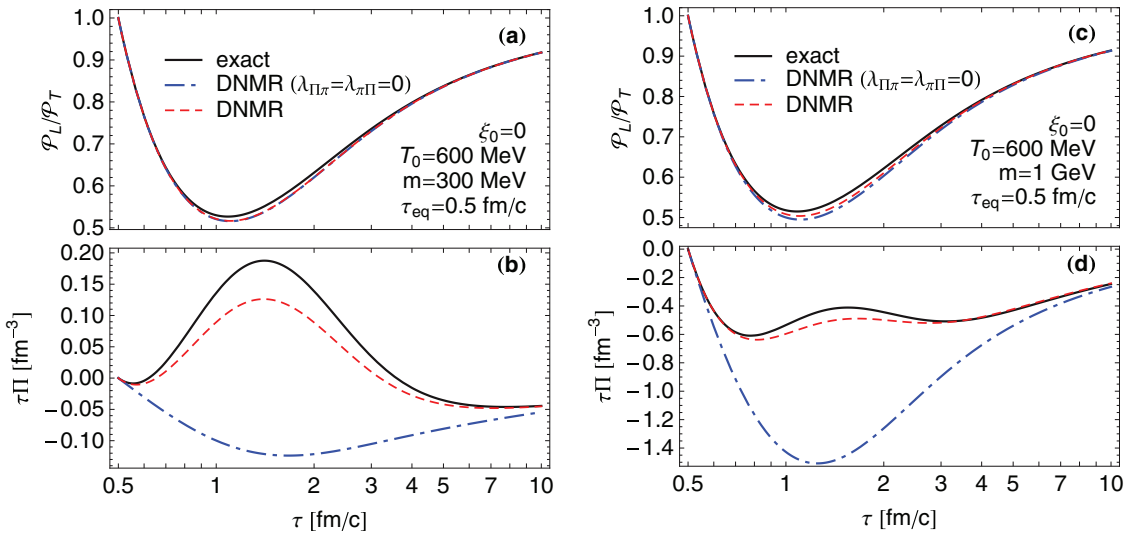

FIG. 2. (Color online) Same as Fig. 1 except here we take $m = 300$ MeV [(a) and (b)] and $m = 1$ GeV [(c) and (d)].

evolution equations. In contrast to traditional viscous hydrodynamics approaches, which make an expansion around the equilibrium state, anisotropic hydrodynamics expands the underlying distribution function around a momentum-space anisotropic state. In this way, the potentially large degree of momentum-space anisotropy in the system is included in the leading order of expansion and treated nonperturbatively. Moreover, in this framework one is not restricted by the condition of being close to the equilibrium state since the dynamical background is allowed to possess even large momentum-space anisotropies.

In its newest formulation [53], the framework of anisotropic hydrodynamics allows for a degree of freedom associated with the bulk pressure of the system. This is accomplished using the following form for the underlying distribution function:

$$f(x,p) = f_{\rm iso}\left(\frac{1}{\lambda}\sqrt{p_\mu\,\Xi^{\mu\nu}\,p_\nu}\right), \tag{25}$$

with $\Xi^{\mu\nu} = u^\mu u^\nu + \xi^{\mu\nu} - \Delta^{\mu\nu}\Phi$, where u^μ is the four-velocity associated with the local rest frame, $\xi^{\mu\nu}$ is a symmetric and traceless tensor, and Φ is the bulk degree of freedom. The quantities u^μ, $\xi^{\mu\nu}$, and Φ are understood to be functions of space and time and obey $u^\mu u_\mu = 1$, $\xi^\mu{}_\mu = 0$, and $u_\mu \xi^{\mu\nu} = 0$.

Taking the isotropic distribution $f_{\rm iso}$ to be a Boltzmann distribution and assuming 0+1D boost-invariant evolution, the dynamics of the system is determined by the three aHydro equations [53]

$$\partial_\tau \log\alpha_x^2\alpha_z + \left[3 + \hat{m}\frac{K_1(\hat{m})}{K_2(\hat{m})}\right]\partial_\tau\log\lambda + \frac{1}{\tau} = \frac{1}{\tau_{\rm eq}}\left[\frac{1}{\alpha_x^2\alpha_z}\frac{T}{\lambda}\frac{K_2(\hat{m}_{\rm eq})}{K_2(\hat{m})} - 1\right]a, \tag{26}$$

$$(4\tilde{\mathcal{H}}_3 - \tilde{\Omega}_m)\partial_\tau\log\lambda + \tilde{\Omega}_T\partial_\tau\log\alpha_x^2 + \tilde{\Omega}_L\partial_\tau\log\alpha_z = -\frac{1}{\tau}\tilde{\Omega}_L, \tag{27}$$

$$\partial_\tau\log\left(\frac{\alpha_x}{\alpha_z}\right) - \frac{1}{\tau} + \frac{3}{4\tau_{\rm eq}}\frac{\xi_z}{\alpha_x^2\alpha_z}\left(\frac{T}{\lambda}\right)^2\frac{K_3(\hat{m}_{\rm eq})}{K_3(\hat{m})} = 0, \tag{28}$$

where $\tau_{\rm eq}$ is the microscopic relaxation time. Above the variables α_i are a particular combination of the traceless (ξ_i) and traceful component (Φ) parts of the underlying momentum-space anisotropy tensor with $\alpha_i = (1 + \xi_i + \Phi)^{-1/2}$. The variable λ is the nonequilibrium energy scale in the distribution function (25) and we have defined two dimensionless mass scales, $\hat{m}_{\rm eq} = m/T$ and $\hat{m} = m/\lambda$. The integrals $\tilde{\mathcal{H}}_3$, $\tilde{\Omega}_T$, $\tilde{\Omega}_L$, and $\tilde{\Omega}_m$ are defined in Eqs. (A3) and (59) of Ref. [53].

Equations (26)–(28) determine the proper-time evolution of α_x, α_z, and λ. The temperature, or, more accurately, the effective temperature appearing above, is determined by requiring energy conservation at all proper times. This results in the dynamical Landau matching condition

$$\tilde{\mathcal{H}}_3\lambda^4 = 4\pi\tilde{N}T^4\hat{m}_{\rm eq}^2[3K_2(\hat{m}_{\rm eq}) + \hat{m}_{\rm eq}K_1(\hat{m}_{\rm eq})]. \tag{29}$$

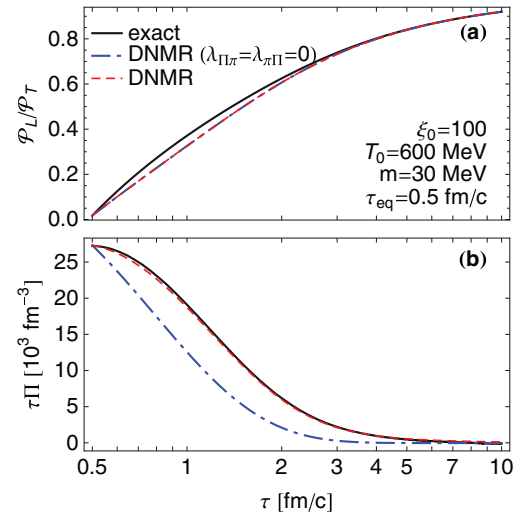

FIG. 3. (Color online) Same as Fig. 1 except here we take $\xi_0 = 100$.

When the system is transversely homogeneous, the longitudinal and transverse pressure can be expressed as

$$\mathcal{P}_T = \tilde{\mathcal{H}}_{3T}(\boldsymbol{\xi},\Phi,\hat{m})\,\lambda^4, \tag{30}$$

$$\mathcal{P}_L = \tilde{\mathcal{H}}_{3L}(\boldsymbol{\xi},\Phi,\hat{m})\,\lambda^4, \tag{31}$$

where $\boldsymbol{\xi} = (\xi_x,\xi_y,\xi_z)$ are the diagonal components of the $\xi^{\mu\nu}$. The $\tilde{\mathcal{H}}_{3T}$ and $\tilde{\mathcal{H}}_{3L}$ functions appearing above are defined by Eqs. (A8) and (A13) in Ref. [53]. Likewise, the bulk pressure can be computed using

$$\Pi(\tau) = \tfrac{1}{3}\left[\mathcal{P}_L(\tau) + 2\mathcal{P}_T(\tau) - 3\mathcal{P}(\tau)\right]. \tag{32}$$

IV. EXACT SOLUTIONS OF BOLTZMANN KINETIC EQUATION IN THE RELAXATION TIME APPROXIMATION

Herein we focus on a transversely homogeneous boost-invariant system. In this case the hydrodynamic flow u^μ should have the Bjorken form in the lab frame $u^\mu = (t/\tau,0,0,z/\tau)$ [62]. This implies that the distribution function $f(x,p)$ can depend only on τ, w, and p_T with $w = tp_L - zE$ [63,64] . Using w and p_L one can define another boost-invariant variable $v = Et - p_L z = \sqrt{w^2 + (m^2 + \vec{p}_T^{\,2})\tau^2}$. Using the boost-invariant variables introduced above, the relaxation time approximation kinetic equation may be written in a simple form,

$$\frac{\partial f}{\partial \tau} = \frac{f_{\rm eq} - f}{\tau_{\rm eq}}, \tag{33}$$

where the boost-invariant form of the equilibrium distribution function is

$$f_{\rm eq}(\tau,w,p_T) = \exp\left[-\frac{\sqrt{w^2 + \left(m^2 + p_T^2\right)\tau^2}}{T(\tau)\tau}\right]. \tag{34}$$

The general form of solutions of Eq. (33) can be expressed as [49,50,52,65–68]

$$f(\tau,w,p_T) = D(\tau,\tau_0) f_0(w,p_T) + \int_{\tau_0}^{\tau} \frac{d\tau'}{\tau_{\rm eq}(\tau')}\, D(\tau,\tau')\, f_{\rm eq}(\tau',w,p_T), \tag{35}$$

where we have introduced the damping function,

$$D(\tau_2,\tau_1) = \exp\left[-\int_{\tau_1}^{\tau_2} \frac{d\tau''}{\tau_{\rm eq}(\tau'')}\right]. \tag{36}$$

For the purposes of this paper, we will assume that at $\tau = \tau_0$ the distribution function f can be expressed in spheroidal Romatschke-Strickland form [69] with the underlying Boltzmann distribution being an isotropic distribution

$$f_0(w,p_T) = \exp\left[-\frac{\sqrt{(1+\xi_0)w^2 + \left(m^2 + p_T^2\right)\tau_0^2}}{\Lambda_0\tau_0}\right], \tag{37}$$

where ξ_0 measures the initial momentum-space anisotropy and Λ_0 is the initial spheroidal momentum scale. This form simplifies to an isotropic Boltzmann distribution if the anisotropy parameter ξ_0 is zero, in which case the transverse momentum scale Λ_0 can be identified with the system's initial temperature T_0. Using Eq. (35) one can derive an integral equation satisfied by the energy density [52]

$$2m^2 T(\tau)[3T(\tau)K_2(\hat{m}_{\rm eq}(\tau)) + mK_1(\hat{m}_{\rm eq}(\tau))] = D(\tau,\tau_0)\Lambda_0^4\tilde{\mathcal{H}}_2\left[\frac{\tau_0}{\tau\sqrt{1+\xi_0}},\frac{m}{\Lambda_0}\right] + \int_{\tau_0}^{\tau}\frac{d\tau'}{\tau_{\rm eq}(\tau')} D(\tau,\tau')T^4(\tau')\tilde{\mathcal{H}}_2\left[\frac{\tau'}{\tau},\hat{m}_{\rm eq}(\tau')\right], \tag{38}$$

where T is the effective temperature which is related to the energy density via Eq. (3). The function $\tilde{\mathcal{H}}_2(y,z)$ above is defined by the integral

$$\tilde{\mathcal{H}}_2(y,z) = \int_0^\infty du\, u^3\, \mathcal{H}_2\left(y,\frac{z}{u}\right)\exp(-\sqrt{u^2+z^2}), \tag{39}$$

with

$$\mathcal{H}_2(y,\zeta) = y\left(\sqrt{y^2+\zeta^2} + \frac{1+\zeta^2}{\sqrt{y^2-1}}\tanh^{-1}\sqrt{\frac{y^2-1}{y^2+\zeta^2}}\right). \tag{40}$$

Equation (38) can be solved numerically using the method of iteration. Using this method, one makes an initial guess for the proper time dependence of the effective temperature, e.g., the ideal hydrodynamics, plugs this into the right-hand side of Eq. (38), and then one solves for the effective temperature necessary to make the left- and right-hand sides equal using a root finder. The resulting effective temperature "profile" is then used as the new "initial guess" and one repeats this process iteratively until the effective temperature profile converges to a given accuracy within the proper-time interval of interest. Once the effective temperature is determined via iterative solution, one can use this to determine the transverse pressure, longitudinal pressure, full distribution function, and so on. For further details, we refer the reader to Ref. [52].

V. RESULTS

In this section we present and discuss our results for the proper-time evolution of the system using different approaches. The results obtained within 14-moment second-order viscous hydrodynamics and anisotropic hydrodynamics are compared with the exact solution. We begin by emphasizing the importance of including the full set of kinetic coefficients in the second-order viscous relativistic hydrodynamics in order to describe the bulk pressure evolution obtained via exact solution of the relaxation time approximation (RTA)

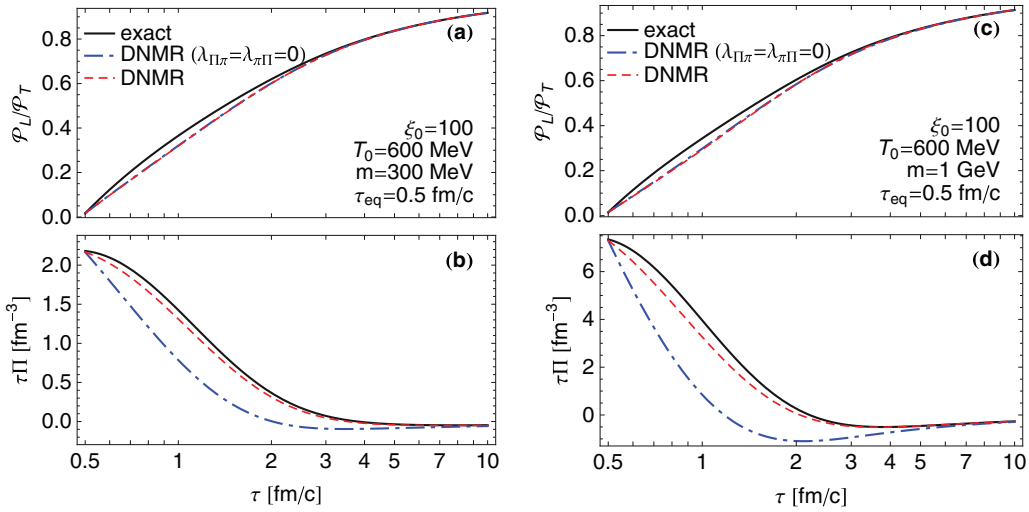

FIG. 4. (Color online) Same as Fig. 2 except here we take $\xi_0 = 100$.

Boltzmann equation. In order to illustrate this point, below we will compare the second-order viscous hydrodynamics predictions with and without the shear-bulk couplings. After making this point, we then compare the results obtained using full second-order viscous hydrodynamics with those obtained within the anisotropic hydrodynamics. We find that the two approaches reproduce the exact solution with comparable accuracy. In all cases we use a fixed relaxation time of $\tau_{\rm eq} = \tau_\pi = \tau_\Pi = 0.5$ fm/c, an initial time of $\tau_0 = 0.5$ fm/c, and an initial temperature of $T_0 = 600$ MeV. We will consider two different initial pressure anisotropies corresponding to an isotropic initial condition ($\xi_0 = 0$) and a highly oblate initial anisotropy ($\xi_0 = 100$). For the particle mass, we will consider three different cases corresponding to $m = 30$ MeV, 300 MeV, and 1 GeV.

A. Shear-bulk couplings in the second-order viscous hydrodynamics

In this section we solve the second-order hydrodynamic equations discussed in Sec. II and compare the obtained solutions with the exact results. In order to have an overlap with our previous results available in the literature, the initial temperature at $\tau_0 = 0.5$ fm/c has been set equal to $T_0 = 600$ MeV. By solving the kinetic equation in the relaxation time approximation using Eq. (38) we obtain the effective temperature $T(\tau)$. As mentioned previously, knowing $T(\tau)$ we can then calculate the exact pressures $\mathcal{P}_L(\tau)$ and $\mathcal{P}_T(\tau)$. We then use Eq. (32) to obtain the exact bulk pressure $\Pi(\tau)$. The exact bulk pressure computed in this manner can be compared directly with the second-order hydrodynamic result for $\Pi(\tau)$, which follows from Eqs. (8)–(10).

In addition, the second-order hydrodynamics results for $\mathcal{P}$, Π, and π can be used to determine $\mathcal{P}_T$ and $\mathcal{P}_L$ via

$$\begin{aligned} \mathcal{P}_L &= \mathcal{P} + \Pi - \pi, \\ \mathcal{P}_T &= \mathcal{P} + \Pi + \pi/2, \end{aligned} \tag{41}$$

In Figs. 1–4 we compare the proper-time evolution of the pressure anisotropy $\mathcal{P}_L/\mathcal{P}_T$ (top panels) and the bulk pressure Π multiplied by proper-time τ (bottom panels) obtained from the exact solution of the Boltzmann equation (black solid line), the full second-order viscous equations including the shear-bulk couplings $\lambda_{\Pi\pi}$ and $\lambda_{\pi\Pi}$ (red dashed line), and second-order viscous equations with $\lambda_{\Pi\pi} = \lambda_{\pi\Pi} = 0$ (blue dot-dashed line). We show the results for two different initial values of the anisotropy parameter $\xi_0 \in \{0, 100\}$ and three values of the particle mass $m \in \{0.03, 0.3, 1\}$ GeV.

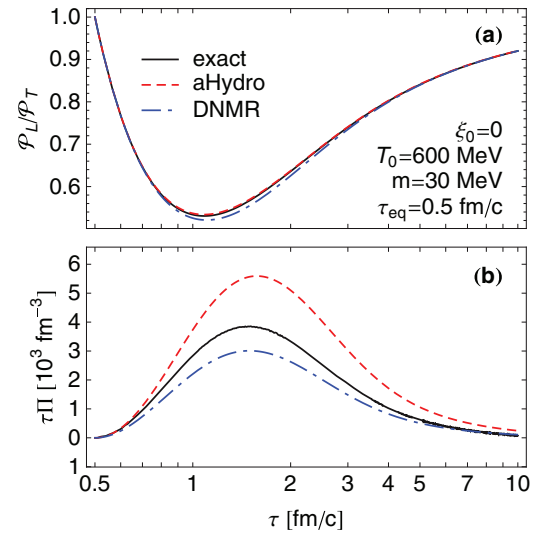

FIG. 5. (Color online) Proper-time evolution of pressure anisotropy $\mathcal{P}_L/\mathcal{P}_T$ (a) and bulk pressure (b). The three lines correspond to the exact solution of the Boltzmann equation [52] (black solid line), the full second-order viscous equations including the shear-bulk couplings $\lambda_{\Pi\pi}$ and $\lambda_{\pi\Pi}$ [32] (blue dot-dashed line), and anisotropic hydrodynamics [53] (red dashed line). For both figures we used $m = 30$ MeV, $\tau_0 = 0.5$ fm/c, $\tau_{\rm eq} = \tau_\pi = \tau_\Pi = 0.5$ fm/c, and $T_0 = 600$ MeV. The initial spheroidal anisotropy parameter for initial distribution function of the exact solution of Boltzmann equation is taken to be $\xi_0 = 0$; in consequence $\pi_0 = 0$ and $\Pi_0 = 0$.

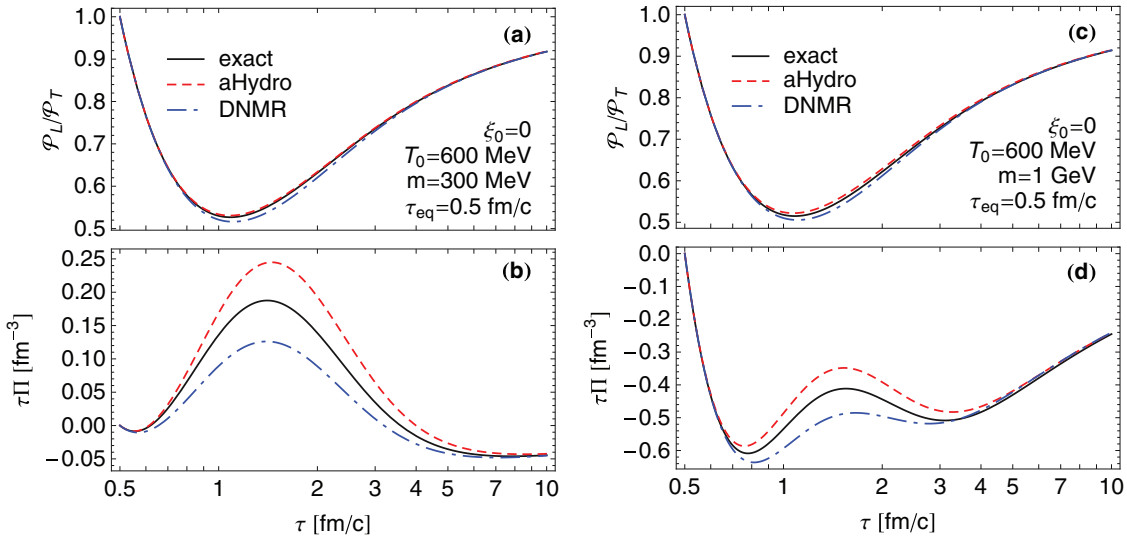

FIG. 6. (Color online) Proper-time evolution of $\mathcal{P}_L/\mathcal{P}_T$ [(a) and (c)] and bulk pressure [(b) and (d)]. Parameters and descriptions are the same as in Fig. 5 except here we take $m = 300$ MeV [(a) and (b)] and $m = 1$ GeV [(c) and (d)].

As one can see from Figs. 1 and 3, which both assume $m = 30$ MeV, the 14-moment second-order viscous hydrodynamical result (DNMR) including the shear-bulk couplings works quite well in reproducing the exact solution for small masses. For the larger masses shown in Figs. 2 and 4 ($m = 300$ MeV and $m = 1$ GeV), we see somewhat larger deviations from the exact solution. Note importantly that in all cases shown, when one turns off the shear-bulk couplings by setting $\lambda_{\Pi\pi} = \lambda_{\pi\Pi} = 0$, the resulting bulk pressure evolution does not agree well with the exact solution demonstrating the importance of these couplings for early time dynamics. Additionally, one notices that inclusion of these couplings has a larger relative effect on the bulk pressure evolution than the pressure anisotropy with the effect on the pressure anisotropy increasing as the mass increases.

Our comparisons between second-order viscous hydrodynamics and anisotropic hydrodynamics are presented in Figs. 5–8. The parameters are chosen to be the same as in the previous section. From these figures, one sees that anisotropic hydrodynamics provides a comparable description of bulk and shear pressure as complete second-order viscous hydrodynamics. However, in the small mass case it seems that second-order viscous hydrodynamics does a better job in reproducing the evolution of the bulk pressure for large initial anisotropies. In most cases, however, anisotropic hydro does a slightly better job in reproducing the exact solution for the pressure anisotropy. Note, however, that herein we have assumed $\tau_{eq} = 0.5$ fm/c in all figures. If one were to take larger values of τ_{eq} or smaller initial temperatures, then one would have to reconsider this comparison.

B. Comparison with anisotropic hydrodynamics

In this section we compare the results of the second-order viscous hydrodynamics and anisotropic hydrodynamics with the exact solutions of the RTA Boltzmann equation. In the framework of anisotropic hydrodynamics the system is characterized by a set of nonequilibrium parameters and one does not deal explicitly with the kinetic coefficients. Interestingly, one may demonstrate that both the second-order viscous hydrodynamics and anisotropic hydrodynamics lead to similar description of the system and the two approaches agree reasonably well with the exact kinetic solution.

Working within the anisotropic hydrodynamics framework, we numerically solve Eqs. (26)–(28) for the nonequilibrium parameters α_x, α_z, and λ. We fix the initial conditions for α_x, α_z, and λ such that the initial energy density, pressure anisotropy, and bulk pressure are the same as those used in the exact solution and the second-order viscous hydrodynamics solution. At each step of the numerical integration we use Eq. (29) to self-consistently determine the effective temperature T which appears in the equations of motion.

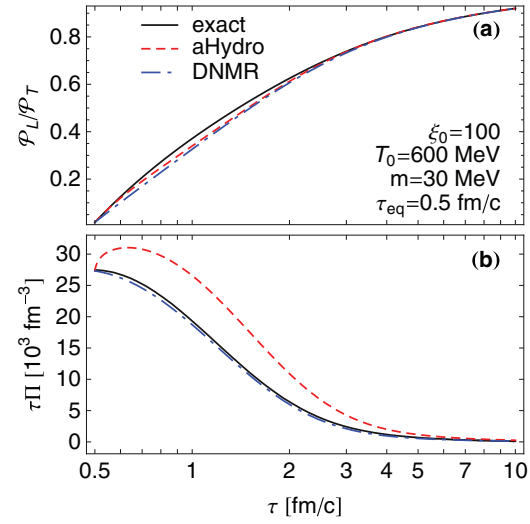

FIG. 7. (Color online) Proper-time evolution of $\mathcal{P}_L/\mathcal{P}_T$ (a) and bulk pressure (b). Parameters and descriptions are the same as in Fig. 5 except here we take $\xi_0 = 100$.

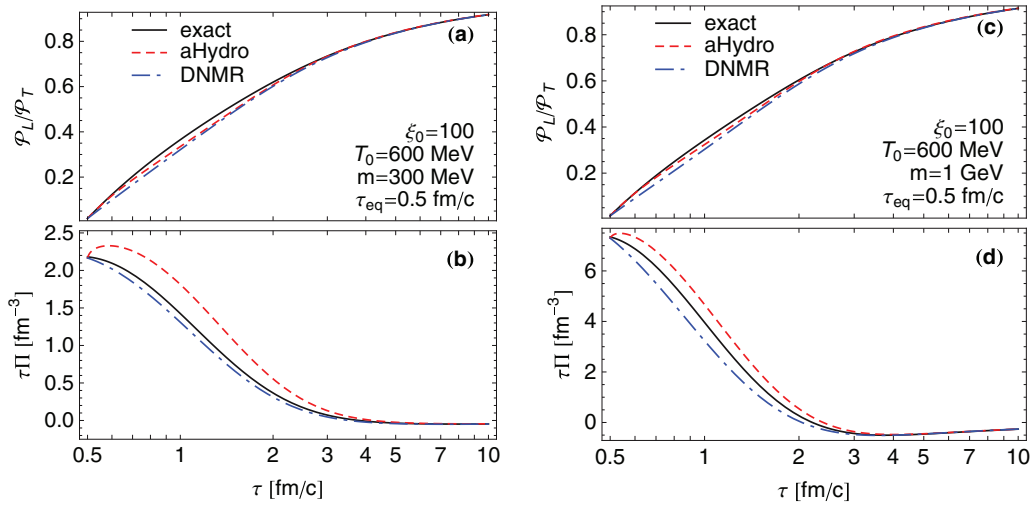

FIG. 8. (Color online) Proper-time evolution of $\mathcal{P}_L/\mathcal{P}_T$ [(a) and (c)] and bulk pressure [(b) and (d)]. Parameters and descriptions are the same as in Fig. 6 except here we take $\xi_0 = 100$.

VI. CONCLUSIONS AND OUTLOOK

In this paper we have demonstrated the importance of shear-bulk coupling in the early time dynamics of the quark-gluon plasma. These couplings are important because there are large shear corrections at early times and these seem to have a marked effect on the evolution of the bulk viscous pressure. The reverse effect of bulk pressure on the shear pressure, measured here in terms of the pressure anisotropy, was found to be small. To reach this conclusion, we compared the results of second-order viscous hydrodynamics using a complete 14-moment approximation with exact solutions to the 0+1D kinetic equations in relaxation time approximation. We found that without the shear-bulk coupling one is not able to reproduce the behavior exhibited by the exact solution.

Following this, we then compared the resulting full 14-moment second-order viscous hydrodynamics results with recently obtained anisotropic hydrodynamics evolution equations which include a bulk degree of freedom. We demonstrated that both the complete second-order viscous hydrodynamics framework and anisotropic hydrodynamics were able to reproduce the exact result with comparable accuracy. For small masses, the 14-moment approximation has better agreement with the bulk pressure evolution than anisotropic hydrodynamics; however, anisotropic hydrodynamics was found to better reproduce the pressure anisotropy in this case. For larger masses, both approaches had comparable accuracy.

Looking forward, herein we showed explicitly that shear-bulk couplings can be important for the early time dynamics of the bulk pressure in simulations of relativistic heavy-ion collisions. It will be interesting to extend the results contained herein to higher-dimensional systems in order to gauge the full impact that shear-bulk couplings have on the dynamical evolution of the system. In the case of anisotropic hydrodynamics, the full 1+1D equations including the effects of the bulk pressure have already appeared in the literature [53]. For 14-moment second-order viscous hydrodynamics, the general equations are known even for 3+1D including bulk viscous effects [32]. It will be interesting to see what the impact shear-bulk couplings will be in both cases. We leave this for future work.

ACKNOWLEDGMENTS

We thank A. Jaiswal for very useful discussions. G.S.D. was supported by a Banting Fellowship from the Natural Sciences and Engineering Research Council of Canada. W.F. was supported by Polish National Science Center Grant No. DEC-2012/06/A/ST2/00390. R.R. was supported by Polish National Science Center Grant No. DEC-2012/07/D/ST2/02125 and US DOE Grant No. DE-SC0004104. M.S. was supported in part by US DOE Grant No. DE-SC0004104.

APPENDIX: THERMODYNAMIC INTEGRALS

The integrals defined in Eq. (24) can be written in the following form:

$$I_{nq}(T,m) = \frac{N_{\rm dof}}{2\pi^2(2q+1)!!}\int_m^\infty e^{-\frac{t}{T}}(t^2-m^2)^{\frac{1}{2}(2q+1)}t^{n-2q}\,dt, \tag{A1}$$

which leads to the following results:

$$I_{-2,0}(T,m) = 4\pi\tilde{N}[K_0(\hat{m}_{\rm eq}) - \hat{m}_{\rm eq}(K_1(\hat{m}_{\rm eq}) - K_{i1}(\hat{m}_{\rm eq}))], \tag{A2}$$

$$I_{-1,0}(T,m) = 4\pi\tilde{N}T\hat{m}_{\rm eq}[K_1(\hat{m}_{\rm eq}) - K_{i1}(\hat{m}_{\rm eq})], \tag{A3}$$

$$I_{0,0}(T,m) = 4\pi\tilde{N}T^2\hat{m}_{\rm eq}K_1(\hat{m}_{\rm eq}), \tag{A4}$$

$$I_{1,0}(T,m) = 4\pi\tilde{N}T^3\hat{m}^2_{\rm eq}K_2(\hat{m}_{\rm eq}), \tag{A5}$$

$$I_{2,0}(T,m) = 4\pi\tilde{N}T^4\hat{m}^2_{\rm eq}(\hat{m}_{\rm eq}K_1(\hat{m}_{\rm eq}) + 3K_2(\hat{m}_{\rm eq})), \tag{A6}$$

$$I_{2,1}(T,m) = 4\pi\tilde{N}T^4\hat{m}^2_{\rm eq}K_2(\hat{m}_{\rm eq}), \tag{A7}$$

$$I_{2,2}(T,m) = 4\pi\tilde{N}\,\frac{T^4\hat{m}^2_{\rm eq}}{30}\big[\big(6-m^2_{\rm eq}\big)K_2(m_{\rm eq}) + m^2_{\rm eq}\big(3K_0(m_{\rm eq}) - 2m_{\rm eq}(K_1(m_{\rm eq}) - K_{i,1}(m_{\rm eq}))\big)\big], \tag{A8}$$

$$I_{3,0}(T,m) = 4\pi\tilde{N}T^5\hat{m}_{\rm eq}\big(\hat{m}_{\rm eq}\big(\hat{m}^2_{\rm eq}+12\big)K_0(\hat{m}_{\rm eq}) + \big(5\hat{m}^2_{\rm eq}+24\big)K_1(\hat{m}_{\rm eq})\big), \tag{A9}$$

$$I_{3,1}(T,m) = 4\pi\tilde{N}T^5\hat{m}^3_{\rm eq}K_3(\hat{m}_{\rm eq}), \tag{A10}$$

$$I_{4,1}(T,m) = 4\pi\tilde{N}T^6\hat{m}_{\rm eq}\big(\hat{m}_{\rm eq}\big(\hat{m}^2_{\rm eq}+20\big)K_0(\hat{m}_{\rm eq}) + \big(7\hat{m}^2_{\rm eq}+40\big)K_1(\hat{m}_{\rm eq})\big), \tag{A11}$$

$$I_{4,2}(T,m) = 4\pi\tilde{N}T^6\hat{m}^3_{\rm eq}K_3(\hat{m}_{\rm eq}), \tag{A12}$$

where $I_{2,1} = \mathcal{P}$, $I_{2,0} = \mathcal{E}$, and $I_{3,0} = T^2(\partial\mathcal{E}/\partial T)$. The function $K_{i,1}(z)$ is defined by the integral

$$K_{i,1}(z) = \int_0^\infty \frac{{\rm e}^{-z\cosh t}}{\cosh t}\,dt, \tag{A13}$$

and can be expressed as [52]

$$K_{i,1}(z) = \frac{\pi}{2}\left[1 - zK_0(z)L_{-1}(z) - zK_1(z)L_0(z)\right], \tag{A14}$$

where L_i is a modified Struve function.

[1] P. Danielewicz and M. Gyulassy, Phys. Rev. D **31**, 53 (1985).
[2] P. K. Kovtun, D. T. Son, and A. O. Starinets, Phys. Rev. Lett. **94**, 111601 (2005).
[3] P. Huovinen, P. F. Kolb, U. W. Heinz, P. V. Ruuskanen, and S. A. Voloshin, Phys. Lett. B **503**, 58 (2001).
[4] T. Hirano and K. Tsuda, Phys. Rev. C **66**, 054905 (2002).
[5] P. F. Kolb and U. W. Heinz, Quark Gluon Plasma 3, edited by R. C. Hwa and X.-N. Wang (World Scientific, Singapore, 2003), pp. 634–714.
[6] A. Muronga, Phys. Rev. Lett. **88**, 062302 (2002).
[7] A. Muronga, Phys. Rev. C **69**, 034903 (2004).
[8] A. Muronga and D. H. Rischke, arXiv:nucl-th/0407114.
[9] U. W. Heinz, H. Song, and A. K. Chaudhuri, Phys. Rev. C **73**, 034904 (2006).
[10] R. Baier, P. Romatschke, and U. A. Wiedemann, Phys. Rev. C **73**, 064903 (2006).
[11] P. Romatschke and U. Romatschke, Phys. Rev. Lett. **99**, 172301 (2007).
[12] R. Baier, P. Romatschke, D. T. Son, A. O. Starinets, and M. A. Stephanov, J. High Energy Phys. 08 (2008) 100.
[13] K. Dusling and D. Teaney, Phys. Rev. C **77**, 034905 (2008).
[14] M. Luzum and P. Romatschke, Phys. Rev. C **78**, 034915 (2008).
[15] H. Song and U. W. Heinz, J. Phys. G **36**, 064033 (2009).
[16] U. W. Heinz, *Relativistic Heavy Ion Physics*, Landolt-Boernstein New Series, I/23, edited by R. Stock (Springer-Verlag, New York, 2010), Chap. 5.
[17] A. El, Z. Xu, and C. Greiner, Phys. Rev. C **81**, 041901 (2010).
[18] J. Peralta-Ramos and E. Calzetta, Phys. Rev. D **80**, 126002 (2009).
[19] J. Peralta-Ramos and E. Calzetta, Phys. Rev. C **82**, 054905 (2010).
[20] G. Denicol, T. Kodama, and T. Koide, J. Phys. G **37**, 094040 (2010).
[21] G. S. Denicol, T. Koide, and D. H. Rischke, Phys. Rev. Lett. **105**, 162501 (2010).
[22] B. Schenke, S. Jeon, and C. Gale, Phys. Rev. Lett. **106**, 042301 (2011).
[23] B. Schenke, S. Jeon, and C. Gale, Phys. Lett. B **702**, 59 (2011).
[24] P. Bozek, Phys. Lett. B **699**, 283 (2011).
[25] H. Niemi, G. S. Denicol, P. Huovinen, E. Molnár, and D. H. Rischke, Phys. Rev. Lett. **106**, 212302 (2011).
[26] H. Niemi, G. S. Denicol, P. Huovinen, E. Molnár, and D. H. Rischke, Phys. Rev. C **86**, 014909 (2012).
[27] P. Bożek and I. Wyskiel-Piekarska, Phys. Rev. C **85**, 064915 (2012).
[28] G. S. Denicol, H. Niemi, E. Molnár, and D. H. Rischke, Phys. Rev. D **85**, 114047 (2012).
[29] G. Denicol, E. Molnár, H. Niemi, and D. Rischke, Eur. Phys. J. A **48**, 170 (2012).
[30] J. Peralta-Ramos and E. Calzetta, Phys. Rev. D **87**, 034003 (2013).
[31] E. Calzetta, arXiv:1402.5278.
[32] G. Denicol, S. Jeon, and C. Gale, arXiv:1403.0962.
[33] W. Florkowski and R. Ryblewski, Phys. Rev. C **83**, 034907 (2011).
[34] M. Martinez and M. Strickland, Nucl. Phys. A **848**, 183 (2010).
[35] R. Ryblewski and W. Florkowski, J. Phys. G **38**, 015104 (2011).
[36] M. Martinez and M. Strickland, Nucl. Phys. A **856**, 68 (2011).

[37] R. Ryblewski and W. Florkowski, Eur. Phys. J. **71**, 1761 (2011).
[38] W. Florkowski and R. Ryblewski, Phys. Rev. C **85**, 044902 (2012).
[39] M. Martinez, R. Ryblewski, and M. Strickland, Phys. Rev. C **85**, 064913 (2012).
[40] R. Ryblewski and W. Florkowski, Phys. Rev. C **85**, 064901 (2012).
[41] W. Florkowski, R. Maj, R. Ryblewski, and M. Strickland, Phys. Rev. C **87**, 034914 (2013).
[42] D. Bazow, U. W. Heinz, and M. Strickland, arXiv:1311.6720.
[43] M. Strickland, arXiv:1312.2285.
[44] W. Florkowski and R. Maj, Acta Phys. Polon. B **44**, 2003 (2013).
[45] L. Tinti and W. Florkowski, Phys. Rev. C **89**, 034907 (2014).
[46] M. Strickland, Nucl. Phys. A **926**, 92 (2014).
[47] W. Florkowski and O. Madetko, Acta Phys. Polon. B **45**, 1103 (2014).
[48] W. Florkowski, R. Ryblewski, M. Strickland, and L. Tinti, Phys. Rev. C **89**, 054909 (2014).
[49] W. Florkowski, R. Ryblewski, and M. Strickland, Nucl. Phys. A **916**, 249 (2013).
[50] W. Florkowski, R. Ryblewski, and M. Strickland, Phys. Rev. C **88**, 024903 (2013).
[51] W. Israel and J. M. Stewart, Ann. Phys. **118**, 341 (1979).
[52] W. Florkowski, E. Maksymiuk, R. Ryblewski, and M. Strickland, Phys. Rev. C **89**, 054908 (2014).
[53] M. Nopoush, R. Ryblewski, and M. Strickland, Phys. Rev. C **90**, 014908 (2014).
[54] E. Molnár, H. Niemi, G. S. Denicol, and D. H. Rischke, Phys. Rev. D **89**, 074010 (2014).
[55] K. Tsumura and T. Kunihiro, Phys. Lett. B **690**, 255 (2010).
[56] A. Monnai and T. Hirano, Nucl. Phys. A **847**, 283 (2010).
[57] A. Monnai, Phys. Rev. C **86**, 014908 (2012).
[58] W. Israel, Ann. Phys. **100**, 310 (1976).
[59] P. Romatschke, Int. J. Mod. Phys. E **19**, 1 (2010).
[60] H. Song and U. W. Heinz, Phys. Rev. C **81**, 024905 (2010).
[61] A. Jaiswal, Phys. Rev. C **87**, 051901 (2013).
[62] J. D. Bjorken, Phys. Rev. D **27**, 140 (1983).
[63] A. Białas and W. Czyż, Phys. Rev. D **30**, 2371 (1984).
[64] A. Białas and W. Czyż, Nucl. Phys. B **296**, 611 (1988).
[65] G. Baym, Phys. Lett. B **138**, 18 (1984).
[66] G. Baym, Nucl. Phys. A **418**, 525 (1984).
[67] H. Heiselberg and X.-N. Wang, Phys. Rev. C **53**, 1892 (1996).
[68] S. M. H. Wong, Phys. Rev. C **54**, 2588 (1996).
[69] P. Romatschke and M. Strickland, Phys. Rev. D **68**, 036004 (2003).